Journal of Clinical Orthopaedics and Trauma xxx (2018) 1–6

Contents lists available at ScienceDirect

Journal of Clinical Orthopaedics and Trauma

journal homepage: www.elsevier.com/locate/jcot

An *in-vitro* animal bone model study to predict spiral fracture strength of long bones in the young infant

S.S. Malik [a], S. Malik [a], R. Shenoy [b], M.D. Jones [a], P.S. Theobald [a, *]

[a] Bioengineering Research Group, Cardiff School of Engineering, Cardiff University, Queens Buildings, The Parade, Newport Road, Cardiff, CF24 3AA, UK
[b] Department of Trauma & Orthopaedics, St Mary's Hospital, Imperial College Healthcare NHS Trust, Praed Street, London, W2 1NY, UK

ARTICLE INFO

Article history:
Received 24 October 2017
Received in revised form
24 September 2018
Accepted 2 October 2018
Available online xxx

Keywords:
Infant
Long bones
Non-accidental injury
Spiral fracture
Torsional fracture strength

ABSTRACT

Introduction: The risk of fracture from a non-accidental injury is highest in the infant age group. A spiral fracture of the long bone can occur equally from accidental and non-accidental causes, meaning the clinical judgement of non-accidental injury in an infant is particularly challenging. This study aimed to assist in differentiating accidental, from non-accidental, injury in infants, by establishing whether correlation exists between geometry and torsional strength in the immature long bone.

Methods: Immature porcine third and fourth metacarpals (n = 21) were imaged with a dual energy x-ray absorptiometry (DEXA) scanner to measure their linear bone mineral content (BMC_L), bone mineral density (BMD) and section modulus (Z). The specimens were then subjected to a torque of one degree per second until failure. The failure strength and the three DEXA measures were analyzed for a correlation.

Results: The mean failure strength of 11 successful tests was 13.71Nm (+/-SD 2.42Nm), with correlation to BMC_L, BMD and Z described by $r^2 = 0.81$, 0.283 and 0.75 respectively.

Conclusion: This study is a novel attempt at estimating torsional strength of long bones in a specific paediatric age group using a size-matched animal bone model. It found a strong correlation between bone and fracture strength parameters over the BMC_L range of 0.59–0.77 g/cm.

1. Introduction

Long bone fractures can be caused by accidental or non-accidental injury. The incidence of fractures in children increases with age,[1] with infants less than one year having the lowest fracture rate. These children are also at a particular risk of fractures from non-accidental injury, due to the circumstances of infancy: they are entirely dependent on their carers, have a limited mobility and are completely defenceless. It is estimated that 40–80% of long bone fractures in this age group may occur through a non-accidental injury.[2] One systematic review stratified the risk according to the long bone fractured, finding that in the absence of an obvious history of relevant trauma or medical condition, there is a 1-in-3 chance of abuse in an infant <18 months with a femoral fracture, and a 1-in-2 chance of abuse in a child <3 years with a humerus diaphysis fracture.[3]

The diagnosis of a non-accidental injury in a child is a subjective decision. It relies on the clinician's judgment considering the given account of injury, clinical assessment and evaluation of fracture. This assessment is complicated by the occurrence of stress fractures and a range of medical conditions that affect the bone strength (e.g. osteogenesis imperfecta). Furthermore, birth related trauma can also result in fractures of the long bones, with a delay in diagnosing the majority of these known to lead to wrongfully suspecting child maltreatment. The reported incidence of post-partum fractures is 0.1–3.5%,[4] although the actual incidence is likely be even higher. The humerus and femur are amongst the most commonly fractured bones from birth-related trauma. Birth-related femoral fractures are reported as 0.13 per 1000 live births, with proximal spiral fractures the most common.[4]

A spiral fracture results from a torsional force acting on the bone. It usually initiates on the bone surface in the mid-diaphysis region of the long bone, which normally has the smallest diameter and therefore is the least stiff. A long bone spiral fracture in the infant had been thought to be strongly suggestive of non-accidental

* Corresponding author. Bioengineering Research Group, Cardiff School of Engineering, Cardiff University, Queens Buildings, The Parade, Newport Road, Cardiff, CF24 3AA, UK.
E-mail addresses: smalik888@googlemail.com (S.S. Malik), shahb.malik@googlemail.com (S. Malik), Shenoy.Ravi@gmail.com (R. Shenoy), JonesMD1@cardiff.ac.uk (M.D. Jones), TheobaldPS@cardiff.ac.uk (P.S. Theobald).

https://doi.org/10.1016/j.jcot.2018.10.001
0976-5662/

injury, but it is now recognised that this fracture can equally occur from innocent injuries and that other fracture patterns may be more common in child mal-treatment.[2] In addition, fractures of the mid-diaphysis of long bones have a relatively low specificity for non-accidental injury as compared with fractures such as ribs, skull fractures and classic metaphyseal lesions. Therefore, the clinical judgement of non-accidental injury in a child <1 year with a long bone spiral fracture is particularly challenging.

This study aims to assist in differentiating accidental, from non-accidental, injury in infants, by establishing whether correlation exists between geometry and torsional strength in the immature long bone. This is achieved by investigating dual energy x-ray absorptiometry (DEXA) derived bone strength parameters and experimentally determined spiral fracture strength, using a representative animal model.

2. Methods

2.1. Selection of animal bone model

The porcine bone model is considered to be an appropriate substitute to human paediatric bone and has been used extensively in research similar to this study. It has equivalent DEXA findings due to similarities in bone size, mass, mineralisation and organization.[5,6] Table 1 shows the radiographic measurements of lengths of the humerus, femur and tibia in an infant up to the age of 6 months.[7] The third and fourth porcine metacarpal bones were found to have a similar length to these measurements and were chosen as the bone model on the basis that the cross-sectional dimensions of an immature bone are a function of the length.[8]

2.2. Specimen preparation

A total of 21 specimens were harvested from fresh pig feet, donated from a commercial abattoir. As these feet were acquired as a consequence of routine slaughter for the food industry, they were exempt from the local ethics process. The metacarpal bones were cleared of all soft tissues and inspected for any previous fractures and obvious defects that could potentially affect the results. The specimens were then wrapped in tissue paper and labelled and stored at 4 °C in a fridge.

2.3. DEXA scan

The specimens were imaged with the QDR Explorer Dual Energy Bone Densitometer (Hologic, USA). Each specimen was placed on a 26 mm plexiglass sheet to simulate the attenuation characteristics of the soft tissues, as previously established by Pierce et al..[9] A lumbar spine acquisition protocol (survey mode) was used, and the scan was analysed using sub-regional spine analysis. The length of one specimen was determined in terms of the number of lines in the image, and correlated with the actual length measured with digital calipers. A 1.5 cm region of interest (ROI), centered on the mid-point of the whole bone, was analysed for BMC (g) and projected area (cm^2) (Fig. 1). These measurements were used to calculate the following indices of bone strength:

Table 1
Radiographic measurements of lengths of long bones in an infant up to the age of 6 months (cm).[7]

	0 months	2 months	6 months
Humerus	6.37	7.20	8.77
Femur	7.65	8.65	11.18
Tibia	6.14	6.95	8.89

- BMC_L (g/cm) was calculated by dividing BMC by the height (h, cm) of ROI i.e. 1.5 cm
- BMD (g/cm^2) was calculated by dividing BMC by the projected area
- Section modulus (Z, cm^3) was calculated using the approximation method of Martin and Burr.[10] This method models the mid-diaphysis as a hollow circular section and assumes that the density of mineral fraction of bone (ρ, g/cm^3) is $3g/cm^3$ and fraction of mineral in cortical bone (K, %) is 35%.[11] According to the method, firstly the cortical cross-sectional area (A, cm^2) is expressed by:

$$A = \frac{BMC}{K\rho}$$

A is then applied in the equation to derive the cross-sectional moment of inertia (I, cm^4). This equation also requires the effective mid-diaphysis periosteal diameter (D, cm) value, which is calculated by dividing the projected area h i.e. 1.5 cm. I is expressed by:

$$I = \frac{A}{4\pi}\left(\frac{\pi}{2}D^2 - A\right)$$

Finally, Z is expressed by:

$$Z = \frac{2I}{D} = \frac{A}{2\pi D}\left(\frac{\pi}{2}D^2 - A\right)$$

Z is an engineering based measure of whole bone resistance to torsion. It takes into account the distribution of material with the bone cross-section and is also a meaningful predictor of bone strength.

2.4. Torsion test

The specimens were thermally equilibrated prior to testing by standing for 2 h in the laboratory (17–19 °C). The porcine metacarpal bone has a growth plate at the distal end, and a common problem in torsion testing of immature bone is the failure of growth plate before the bone is fractured, because the connective tissues are weaker than the cortical bone. Therefore, a 3 mm diameter bicortical hole was drilled adjacent to the growth plate and a metal pin was inserted across the bone, creating a pair of extensions, which once fixed in the potting material prevented torsion being applied across the growth plate during the test. Fourteen specimens were tested with this preparation. The technique was then adapted and a 1.5 mm unicortical hole with only one metal pin extension was found to be equally effective in resisting growth plate torsion. Seven specimens were tested with the modified preparation.

The proximal and distal ends of each metacarpal bone were then embedded in steel jigs filled with Woods metal. Once potting was complete, each specimen was mounted into an MTS 858 Mini Bionix® II Test Machine (MTS Systems Corporation, USA) with torsional and axial loading capabilities (Fig. 2). It was ensured that the specimens were vertically aligned in the machine, so that the torque was applied to the long axis of the bone and did not induce a bending moment. The working length (cm) of each specimen was measured with a ruler; this was defined as the bone length exposed between the embedded ends.

Axial load was maintained at zero and a torque of one degree per second was applied. Torque (Nm) and angular displacement (deg) were recorded at 10 Hz and the test was stopped at specimen failure. After the test, the specimens were recovered and examined to determine whether the fracture line included the hole of the 'derotational' pin, whilst the angle of spiral fracture to the

Please cite this article in press as: Malik SS, et al., An *in-vitro* animal bone model study to predict spiral fracture strength of long bones in the young infant, Journal of Clinical Orthopaedics and Trauma (2018), https://doi.org/10.1016/j.jcot.2018.10.001

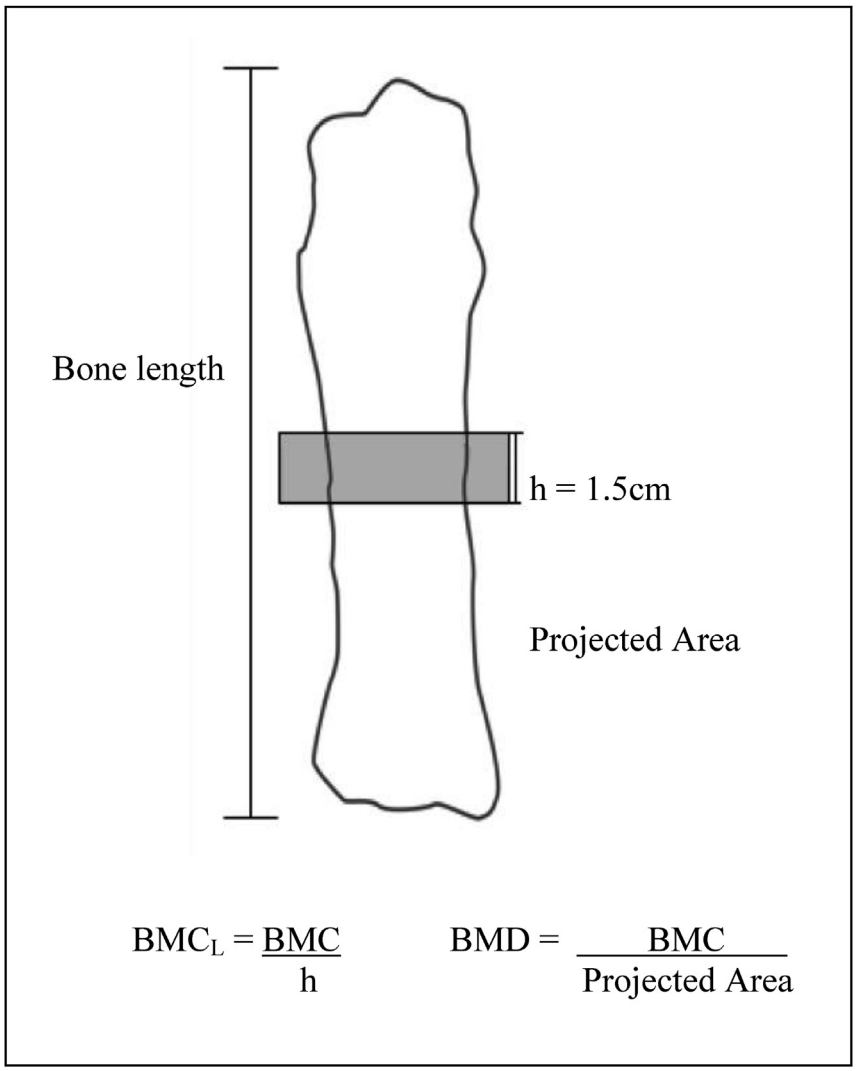

Fig. 1. A drawing of a typical porcine third and fourth metacarpal with DEXA measurements indicated. A 1.5 cm height ROI centred over the mid-diaphysis was analysed for projected area and BMC.

longitudinal axis of the bone was also measured.

2.5. Statistics

All data were collected and analysed using Excel spreadsheets (Microsoft Corp, Seattle, WA) and GraphPad Prism® 5.01(GraphPad software Inc.). Correlation between parameters was assessed with Pearson's test and the r squared values calculated. Significance in differences between two correlation coefficients was calculated using a Fishers r-to- z transformation. $p < 0.05$ was considered significant.

3. Results

All 21 specimens failed with a spiral fracture. None of the specimens failed at the growth plate, but the fracture involved the drill hole in eight of fourteen specimens tested with a 3 mm bicortical hole with a metal pin and two of seven specimens tested with 1.5 mm unicortical hole with a metal pin. Although the derotational pin and pin holes were embedded in the potting material and did not contribute to the working length of bone, the results of the specimens in which the fracture line involved the drill hole were excluded from the analysis, due to the uncertainty of whether the fracture initiated from the stress riser created by the hole.

The remaining 11 metacarpal bones had a mean length of 7.40 cm (+/-SD 0.32 cm) and a mean mid-diaphysis periosteal diameter of 1.68 cm (+/-SD 0.09 cm). Table 2 shows their DEXA-derived indices of bone strength. The mean working length was 2.90 cm (+/-SD 0.39 cm). Fig. 3 shows the load-displacement curve for specimen no. 1, which is typical of all the specimens tested. There is an initial linear region of elastic deformation, then a non-linear region of plastic deformation that reaches a maximum failure load at which the bone fails. The gradient of the initial linear region indicates the torsional stiffness, and the maximum torque before failure indicates the structural strength of the whole bone. The angular deformation was converted from degrees to radians for calculating torsional stiffness. The area under the curve indicates the energy absorbed to failure. This was calculated using the trapezoidal method. Table 3 shows the torsional strength test results for these specimens. The mean angle of the spiral fracture to the long axis of the bone was 30.40° (+/-SD 5.86°).

The correlations of the different DEXA-derived indices of bone strength with maximum torque are shown in Figs. 4–6. There was a strong correlation between BMC_L and maximum torque ($r^2 = 0.805$,

Please cite this article in press as: Malik SS, et al., An *in-vitro* animal bone model study to predict spiral fracture strength of long bones in the young infant, Journal of Clinical Orthopaedics and Trauma (2018), https://doi.org/10.1016/j.jcot.2018.10.001

Fig. 2. A specimen embedded in the steel jigs and positioned in the test machine.

Table 2
The DEXA-derived indices of bone strength [mean (+/-SD)] (n = 11).

BMC_L (g/cm^2)	BMD (g/cm^2)	Z (cm^3)
0.72 (0.08)	0.43 (0.03)	0.33 (0.04)

$p = 0.0002$). There was also a strong correlation between Z and maximum torque ($r^2 = 0.751$, $p = 0.0006$). The difference between the correlation coefficients was not significant ($p = 0.78$), indicating that both indicators predicted strength equally well. There was only a weak correlation between BMD and maximum torque, which was not significant ($r^2 = 0.283$, $p = 0.092$).

4. Discussion

This study used an immature porcine metacarpal bone model to replicate spiral fracture of a long bone in a young infant. It is a novel approach to predicting torsional strength of long bones in a specific paediatric age group using a size-matched animal bone model. Within the limitations of the *in-vitro* testing techniques, the findings of this study provide an estimation of the likely torsional strength of the long bones in the young infant. The mean maximum torsion load for the animal bone model was 13.71Nm (SD± 2.42Nm). All specimens experienced a spiral fracture that was representative of the fracture pattern clinically found in paediatric torsional trauma situations. The angle of the spiral fracture was 30.40° (SD±5.86°), which is consistent with the findings of previous experimental studies[10,12] and with the fracture angle observed clinically.[13]

This study found that Z was comparable to, but not better than, BMC_L in the ability to predict whole bone torsional strength. These findings are similar to the work of Sarin et al.[14] who also compared the same correlations in the femora of different species, covering a BMC_L range of 0.91–6.1 g/cm. The BMC_L range of the specimens tested in the present study was 0.59–0.77 g/cm. This study therefore extends the BMC_L range over which the DEXA-derived strength indicators have been validated in an *in-vitro* torsional strength test. In the work by Sarin et al.,[14] the correlation of BMC_L and Z with strength was $r^2 = 0.87$ and $r^2 = 0.86$, respectively. In the present study, the correlation of BMC_L and Z with strength was $r^2 = 0.81$ and $r^2 = 0.75$, respectively. Although the relative ability of the two indices to predict torsional strength was the same as previously reported, both indices had a lower correlation with strength. The difference in the indicators' correlation with strength in the two studies is explained by the differences in the cross-sectional geometry, especially circularity and wall thickness, of the bones tested in the two studies, and the different values of fraction of mineral in cortical bone, K, used in the calculations of the studies. Sarin et al.[14] estimated K to be 42%, whereas the present study used

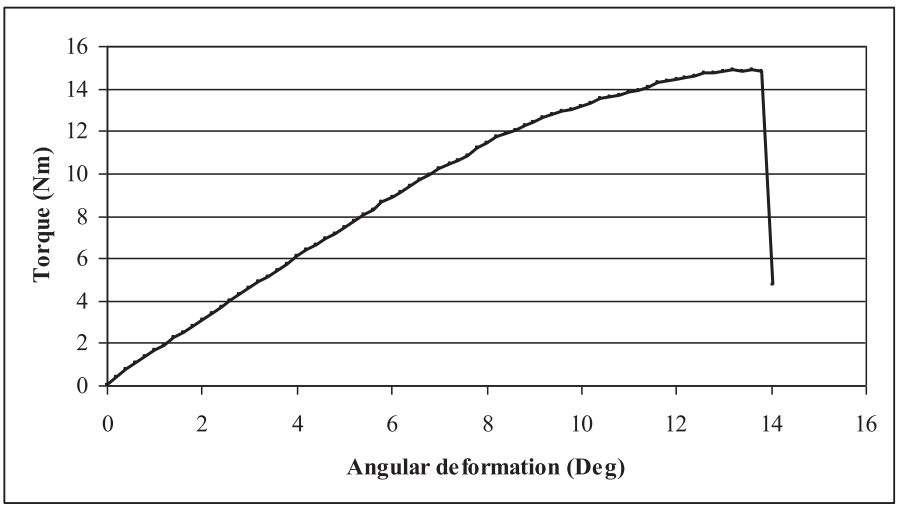

Fig. 3. Load deformation curve for specimen 1.

Please cite this article in press as: Malik SS, et al., An *in-vitro* animal bone model study to predict spiral fracture strength of long bones in the young infant, Journal of Clinical Orthopaedics and Trauma (2018), https://doi.org/10.1016/j.jcot.2018.10.001

Table 3
Torsional strength test data [mean (+/-SD)] (n = 11).

Max torque (Nm)	Angular deformation (deg)	Torsional stiffness (Nm/rad)	Energy absorption (Nm.deg)
13.71 (2.42)	19.15 (4.66)	60.89 (15.21)	191.38 (67.41)

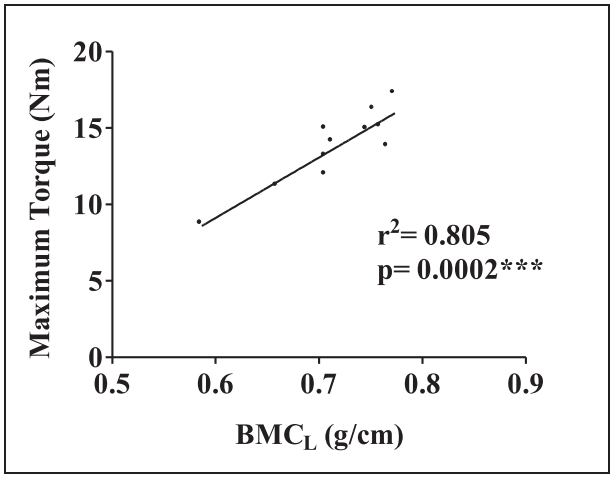

Fig. 4. The correlation of BMC $_L$ with maximum torque.

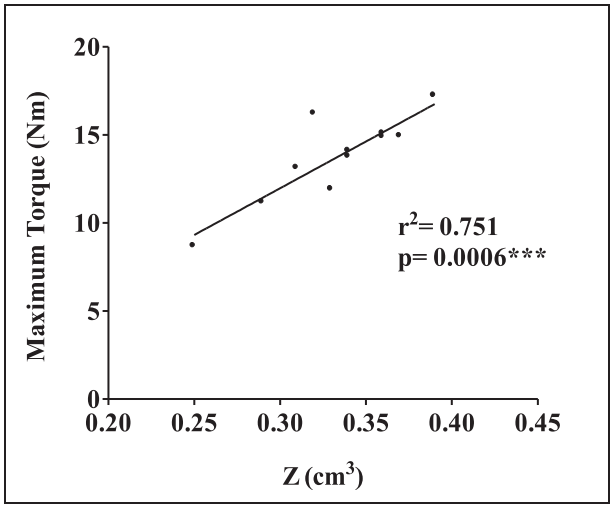

Fig. 5. The correlation of Z with maximum torque.

the K value of 35%, as estimated by Martin and Burr[10] and used by other researchers.[15]

Based on the engineering principles, Z might be expected to be a better predictor of torsional strength than BMC$_L$. Z takes into account the contribution of the cross-sectional geometry to the whole bone structural strength. These geometric effects are critical in children, because in the growing skeleton the bone cross-sectional geometry is a function of its length.[8] Therefore, as the paediatric bone increases in length, there is a compensatory increase in the cross-sectional dimensions to maintain strength.[8] On the other hand, BMC$_L$ is also linearly related to the bone cross-section area.[8,14] The calculations for deriving Z contain empirical constants, ρ and K, which would weaken the accuracy of Z compared with BMC$_L$, which is directly related to the cross-sectional area. The small sample size assessed in this study may not have enough power to differentiate between the two parameters of strength.

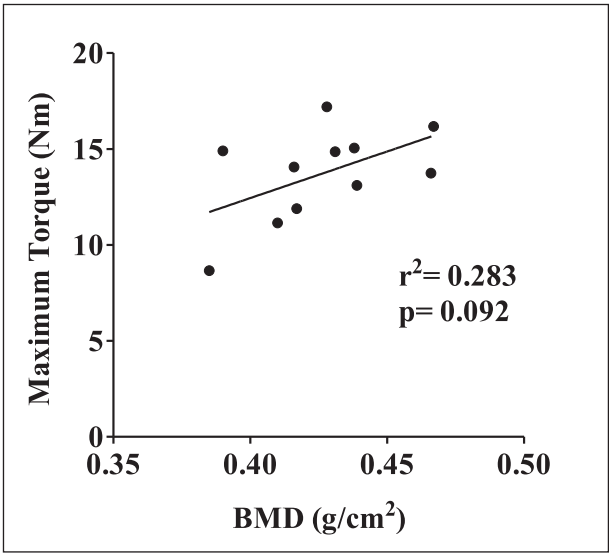

Fig. 6. The correlation of BMD with maximum torque.

The embedment of the bone ends in the jig containers for placement in the torsional strength test machine resulted in a considerably reduced working length as compared with the bone length. Ho et al.[16] used the same specimen potting technique in their torsional strength test of mature porcine femora. Table 4 shows a comparison between the bone length and working length of specimens tested in the two studies. This methodology for specimen placement in the torsional strength test machine is associated with a considerable loss of bone length for the actual test. In the present study the percentage working length of the specimens is even shorter because the skeletally immature specimens had to be embedded deeper to protect the growth plate. However, according to the engineering principles the torsional strength of a material is related to the material and cross-sectional properties, but is independent of its length (the angular deformation before failure increases with working length but the material fails at the same maximum torsional load).[17,18] In the present study, the short working length limited the effect of the changing cross-sectional geometry along the bone length on the results obtained.

Several assumptions were made in this study that have a bearing on interpretation of the findings. It was assumed that the cross-section geometry of the porcine bone model is comparable to the cross-sectional geometry of the long bones in the infant. Osteological research provides information on the cross-sectional morphology of the tibia, femur and humerus of the infant. The tibia has a triangular cross-section at the proximal end and diaphysis due to the distinct anterior crest, and square or rhomboid cross-section at the distal end.[19] The femur is always longer than tibia at any developmental stage, and has a rounder cross-section than that of tibia. As the linea aspra develops, it adapts the shape of a teardrop rather than triangular like the tibia.[19] The humerus is round at the proximal end and diaphysis, and is flattened at the distal end. In early infancy the epiphyses of these long bones are similar in size and shape.[19] Fig. 7 shows the computed tomography image of the mid-diaphysis of one of the specimens tested. The

Please cite this article in press as: Malik SS, et al., An *in-vitro* animal bone model study to predict spiral fracture strength of long bones in the young infant, Journal of Clinical Orthopaedics and Trauma (2018), https://doi.org/10.1016/j.jcot.2018.10.001

Table 4
A comparison between bone length and working length of specimens tested in this study and a study by Ho et al.[16].

	Present study	Data from Ho et al.[16]
No of specimens tested	11	40
Bone length [mean (+/-SD)]	7.40 (0.33)	19.24 (0.44)
Working length [mean (+/-SD)]	2.9 (0.39)	10.27 (0.3)
Mean working length as a proportion of bone length	39.19%	53.38%

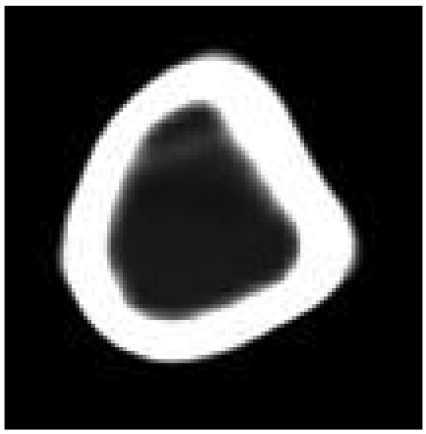

Fig. 7. A computed tomographic image at the mid-diaphysis of the porcine metacarpal bone.

cross-sectional geometry, being approximately circular, is generally similar to that of the long bones of the infant. Further work is also required to show the correlation between this methodology and the long bones in an infant.

Additional limitations of the study include that single torque of one degree per second was tested, adopted from previous studies.[9,14] However, this torque is not based on any specific clinical evidence, and the effect of a change in torque has not been studied. The *in-vitro* experiments produce specific fractures under controlled loading conditions, but the fractures seen clinically are produced by complex loading conditions and therefore the experimental findings have limited applicability. Also, the tested specimens had the soft tissues removed and the effect of the surrounding soft tissues on bone torsional strength properties has not been studied. The experiment technique successfully produced spiral fractures in the specimens, but almost half of the tested specimen had to be excluded from the main analysis because their fractures involved the drill hole for the derotational metal pin. The adapted technique of using a 1.5 mm unicortical hole filled with a derotational pin showed promise in reducing the proportion of fractures affected by the drill hole.

5. Conclusions

This exploratory study used an immature porcine metacarpal bone model to replicate a long bone spiral fracture in an infant. It is a novel attempt at characterising torsional strength of long bones of an infant using a size-matched animal bone model. The study found a strong correlation between bone and fracture strength parameters over the BMC_L range of 0.59–0.77 g/cm. Further studies are required to allow application of these findings to the long bones of the infant.

Acknowledgements

We thank Dr Chee Gan and the radiology staff at the University Hospital of Wales, Cardiff, for performing the radiological studies.

References

1. Rennie L, Court-Brown CM, Mok JYQ, Beattie TF. The epidemiology of fractures in children. *Injury*. 2007;38:913–922.
2. Pierce MC, Bertocci GE, Vogeley E, Moreland MS. Evaluating long bone fractures in children: a biomechanical approach with illustrative cases. *Child Abuse Neglect*. 2004;28:505–524.
3. Kemp AM, Dunstan F, Harrison S, et al. Patterns of skeletal fractures in child abuse: systematic review. *BMJ*. 2008;337:a1518.
4. Bilo RAC, Robben SGF, Van Rijn RR. *Forensic Aspects of Pediatric Fractures: Differentiating Accidental Trauma from Child Abuse*. London: Springer; 2009.
5. Aerssens J, Boonen S, Lowet G, et al. Interspecies differences in bone composition, density and quality: potential implications for in vivo bone research. *Endocrinology*. 1998;139:663–670.
6. Brunton JA, Weiler HA, Atkinson SA. Improvement in the accuracy of dual energy x-ray absorptiometry for whole body and regional analysis of body composition: validation using piglets and methodologic considerations in infants. *Pediatr Res*. 1997;41:590–596.
7. Angel JL. *The People. Lerna II. Gluckstadt (Germany)*. vol. 92. National museum of natural history; 1971.
8. Petit MA, Beck TJ, Kontulainen SA. Examining the developing bone: what do we measure and how do we do it? *J Musculoskelet Neuronal Interact*. 2005;5:213–224.
9. Pierce MC, Valdevit A, Anderson, et al. Biomechanical evaluation of dual-enery x-ray absorptiometry for predicting fracture loads of the infant femur for injury investigation: an in vitro porcine model. *J Orthop Trauma*. 2000;14:571–576.
10. Martin RB, Burr DB. Non-invasive measurement of long bone cross-sectional moment of inertia by photo absorptiometry. *J Biomech*. 1984;17:195–201.
11. Robinson RA. Physicochemical structure of bone. *Clin Orthop*. 1975;112:263–315.
12. Peterson DL, Skraba JS, Moran JM, Greenwald AS. Fractures of long bones: rate effects under singular and combined loading states. *J Orthop Res*. 1984;1:244–250.
13. Morgan EF, Bouxsein ML. Biomechanics of bone and age-related fracture. In: Bilezikian JP, Raisz LG, Martin TJ, eds. *Principles of Bone Biology*. third ed.. London: Elsevier; 2008:29–52; vol. 1.
14. Sarin VK, Polefka EGL, Beaupre GS, et al. DXA-derived section modulus and bone mineral content predict long-bone trosional strength. *Acta Orthop Scand*. 1999;70:71–76.
15. van der Meulen MCH, Ashford Jr MW, Kiratli J, et al. Determinants of femoral geometry and structure during adolescent growth. *J Orthop Res*. 1996;14:22–29.
16. Ho KWH, Gilbody J, Jameson T, Miles AW. The effect of 4mm cortical drill hole defect on bone strength in a pig femur model. *Arch Orthop Trauma Surg*. 2010;130:797–802.
17. Jayaram MA. *Mechanics in Materials with Programs in C*. New Delhi: Prentice-Hall; 2007.
18. Bertocci G. Long bone fracture biomechanics. In: Carole J, ed. *Child Abuse and Neglect: Diagnosis, Treatment and Evidence*. Canada Elsevier; 2011.
19. Baker BJ, Dupras TL, Tocheri MW: The Osteology of Infants and Children. Texas: A&M University Press. 118.

Please cite this article in press as: Malik SS, et al., An *in-vitro* animal bone model study to predict spiral fracture strength of long bones in the young infant, Journal of Clinical Orthopaedics and Trauma (2018), https://doi.org/10.1016/j.jcot.2018.10.001